

**A COMPARATIVE EVALUATION OF RATIO TRANSFORMED  
AND ENHANCED THEMATIC MAPPER IMAGES IN LANDCOVER  
CLASSIFICATION OF THE SAHEL REGION OF WEST AFRICA**

**Igbokwe, J. I.\***  
Institute for Photogrammetry  
and Engineering surveys  
University of Hannover  
Germany.  
(ISPRS Commission VII)

**ABSTRACT:**

A window of 512 X 512 pixels taken from TM image of Tahoua area of Niger Republic, acquired on 3rd September 1989 was corrected for Atmospheric effects. Principal component analysis was used to select bands for further processing. Band ratioing was applied to the selected bands on one hand to generate 4 ratio composite images while spatial filtering (LP-filtering, directional HP-filtering and undirectional HP-filtering) was applied to the selected bands on the other hand to generate a new multispectral image. Training sites were selected from both the ratio composites and the new multispectral image. A supervised classification technique was used to generate 5 landcover classification maps of the study area. A comparative analysis of the classified maps was made to evaluate the performance of each of the images, in discriminating a given class from the others. The aim was to see which of the images so formed will provide a more acceptable result in studying and mapping landcover changes in this region.

**KEY WORDS:** Introduction, Data acquisition, Image transformations, Classification, Analysis of results

**1. INTRODUCTION**

The Sahel region of West Africa is covered mainly by tree dotted annual grass savanna. Apart from major towns, where the population concentration is high, the vast area is inhabited by nomadic people who engage in subsistence farming and migratory herding. Rainfall is usually very short, lasting between 2 and 4 months. Draught, desertification, soil erosion and human activities are the major environmental problems affecting this region. Over the years the effects of these phenomena have caused large changes in the nature of the landcover.

In the past it has been difficult to effectively monitor the effects of these phenomena because of lack of suitable, timely and accurate mapping. Fortunately advances in Remote Sensing technology have provided effective means of gathering information about the environment. Satellite images are now being employed to obtain medium and small scaled thematic maps of different parts of the Earth. Landsat TM data have been used extensively in landcover mapping and in other related studies. Examples of such studies can be found in Chalmers et al (1981), Congalton et al (1983), Irons et al (1985), Hill and Megier (1986), Ioka and Koda (1986), Dech (1987), Dreiser (1988), LaBash and Civco (1989), Schumacher (1991).

The 'Gesellschaft für Angewandte Fernerkundung' in Munich Germany (1991) also performed thematic mapping of Mayo-Kebbi and Ouaddai Biltine areas of Chad Republic using both Landsat and Spot data.

In landcover classification, different methods have been employed to enhance the accuracy of classification. Most of these methods involve linear and statistical transformations. Common transformations are band ratioing, vegetation indices, principal component analysis and tasseled cap transformations (LaBash and Civco 1989). Such transformations help to reduce the redundancy in spectral information and to normalise the effects of natural scene variation caused by atmospheric effects (Jenson 1986, LaBash and Civco 1989). Various researchers have also carried out studies aimed at the evaluation of the effects of each of these transformations in landcover / landuse classifications and in change detection. Examples of such studies include Chalmers and Haris (1981), Fung and LeDrew (1987), Pinter et al (1987), LaBash and Civco (1989). Spatial filtering operations are also used to enhance satellite images before classification. Common filtering operations are low-pass filtering which deemphasizes high spatial frequency details and retains low frequency components, high-pass filtering which is used to remove slowly varying components and retain high frequency ones. Others are linear and non-linear edge enhancements, which emphasize lines and edges in the images (Jenson 1986). The emphasis in this paper is on ratio transformed and enhanced TM images. The objectives of this study are:

\* Mr. Igbokwe, J. I. is a graduate researcher under Prof. (Dr.) G. Konecny at the Institute for Photogrammetry and Engineering Surveys, University of Hannover, Germany.

- i) To generate landcover classification maps of the study area using both the ratio composite and the enhanced TM images.
- ii) To evaluate the performance of each of the ratio composites and the enhanced image in supervised landcover classification.
- iii) Based on the above to determine which of the images so formed will give a better result when studying the landcover changes in this region.

## 2. STUDY AREA

The study area for this investigation is situated near the town of Tahoua in the south western Niger Republic. It has an area of about 235.93 km<sup>2</sup>, which is equivalent to 512 X 512 pixels of 30m TM spectral resolution. It lies approximately 5° 35' to 5° 45' W longitude and 14° 40' to 14° 50' N latitude (fig. 1). The vegetation is made up of mainly grass savanna and shrubs near the water sources. The water potential is not very high. The area has small rivers, seasonal streams and flood plains that are fed by rain during the rainy seasons.

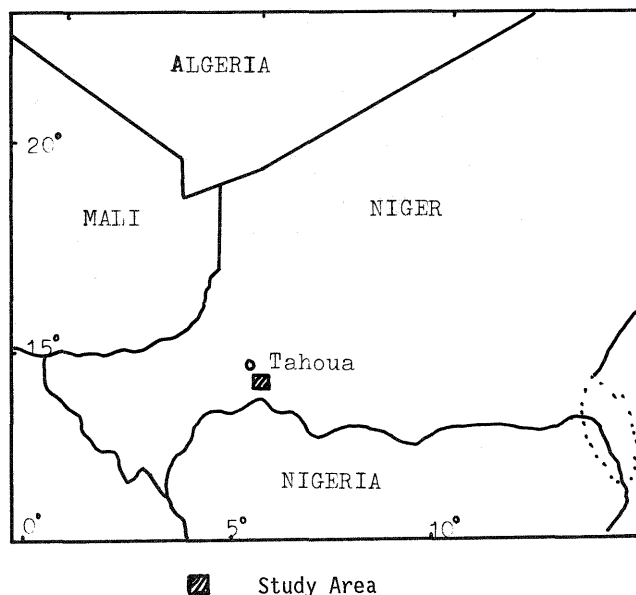


Fig. 1 Approximate location of the study area.

## 3. DATA ACQUISITION

Landsat TM 4 image from path 089 and row 256 was used. The scene was acquired on 3rd September 1989, towards the end of rainy season. Figure 2 shows a colour composite of the study area, made up of channels 7, 4, 1, assigned to red, green and blue respectively. Ancillary data such as aerial photographs and topographical maps (1:50 000) were also used.

## 4. IMAGE PROCESSING

The procedure adopted for this study is illustrated on the flow chart on fig. 3. The image processing was done with GOP 302 image processing system at the Institute for Photogrammetry and Engineering Surveys, University of Hannover Germany. After windowing, atmospheric correction and bands selection, the selected bands were then transformed in two ways. Firstly band ratioing was used to generate 4 ratio composite images and secondly spatial filtering operation was used to generate a new multispectral image. Each of the steps taken will be discussed below.

### 4.1 Image correction

A window of 512 X 512 pixels study site was used. It consisted of bands 1 to 5 and 7. Band 6 was not used because of its lower spatial resolution of 120m (Konecny and Lehmann 1984, LaBash and Civco 1989). Atmospheric correction was applied to suppress the effects of haze. The correction was done through histogram adjustments, based on a subtractive bias established for the band being corrected. The result-

tant image was then normalised.

### 4.2 Principal component analysis

Principal component analysis was used mainly to reduce the redundancy in the original bands. After the transformation the first three components cumulatively accounted for over 99% of the total variance. To select suitable bands for further processing while avoiding loss of spectral infor-

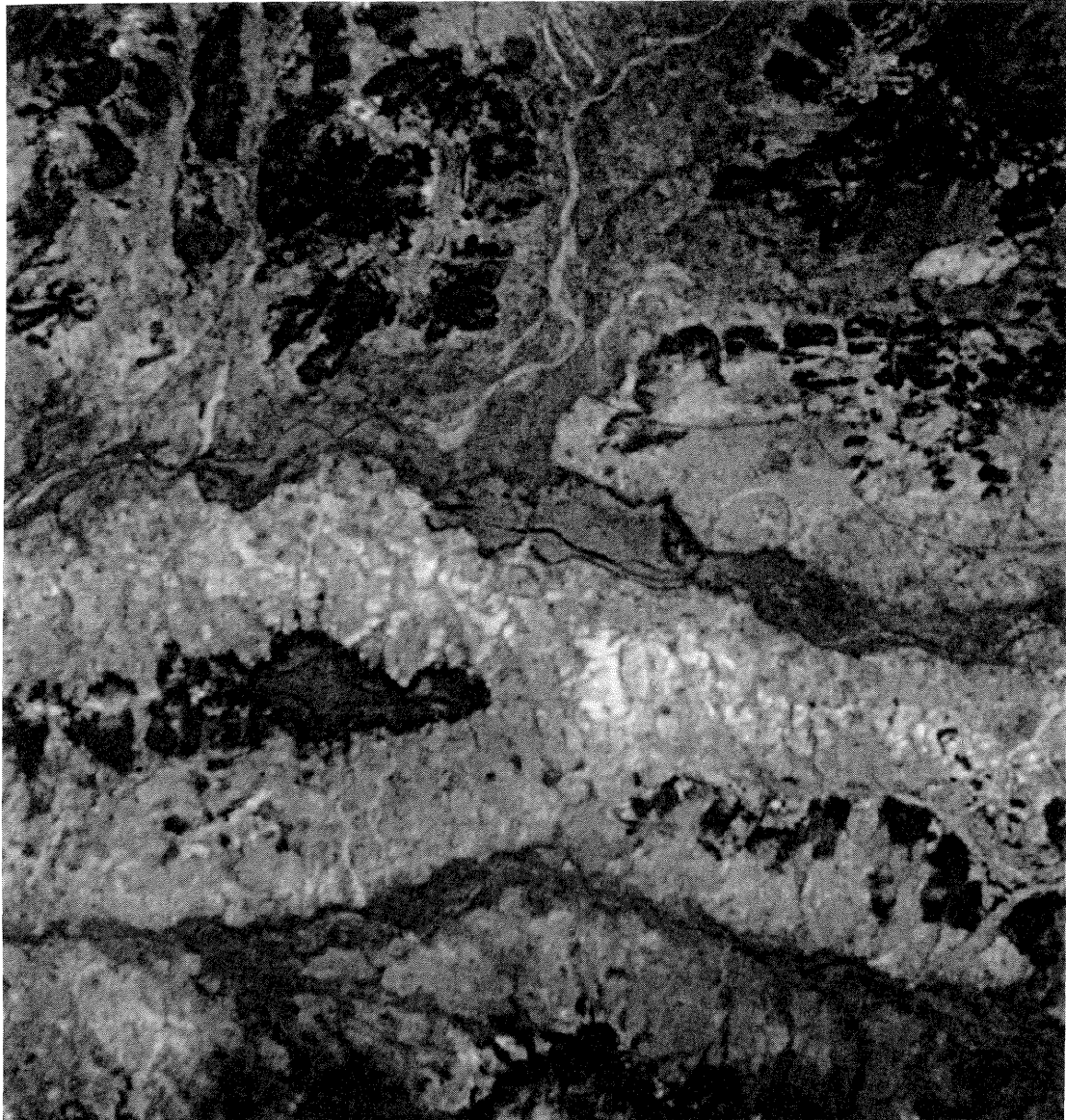


Fig.2 Colour composite of the study area (Bands 7 /4 /1 ) After atmospheric correction

mation, the correlation of each band with each component was computed. The computation was done with the formula (1).

$$R(k,p) = \frac{A(k,p) \times \sqrt{\lambda_p}}{\sqrt{\text{VAR}(k)}} \quad (1)$$

where  $A(k,p)$  is the eigenvector for band  $k$  and component  $p$ ,  
 $\lambda_p$  -  $p$ th eigenvalue (component)  
 $\text{VAR}(k)$  - variance of band  $k$  in the variance-covariance matrix of the image set.

Through this it was possible to determine how each band loads each of the first three components (Jenson 1986). Based on this assessment, bands 1, 3, 4, and 7 were selected. This combination contained at least one band in each of the major spectral wavelengths and can provide ideal separability in landcover classification.

#### 4.3 Band ratioing

Four ratio composite images were generated with the selected bands of the original image. The ratio composites were assigned the names TR1, TR2, TR3 and TR4 respectively. Each composite consists of 3 ratio combinations. The ratios were computed based on the normalising function (2) which encodes the ratio values from 0 to 255 (Jenson 1986).

$$(P_{i,j})_{\text{norm}} = C \left( \arctan \frac{(P_{i,j})_k}{(P_{i,j})_l} \right) \quad (2)$$

where  $C$  is a constant equal to 162.34  
 $(P_{i,j})_k$  and  $(P_{i,j})_l$  are the pixel values in position  $i, j$  in bands  $k$  and  $l$  respectively.  
 The generated ratio composite images are as follows:

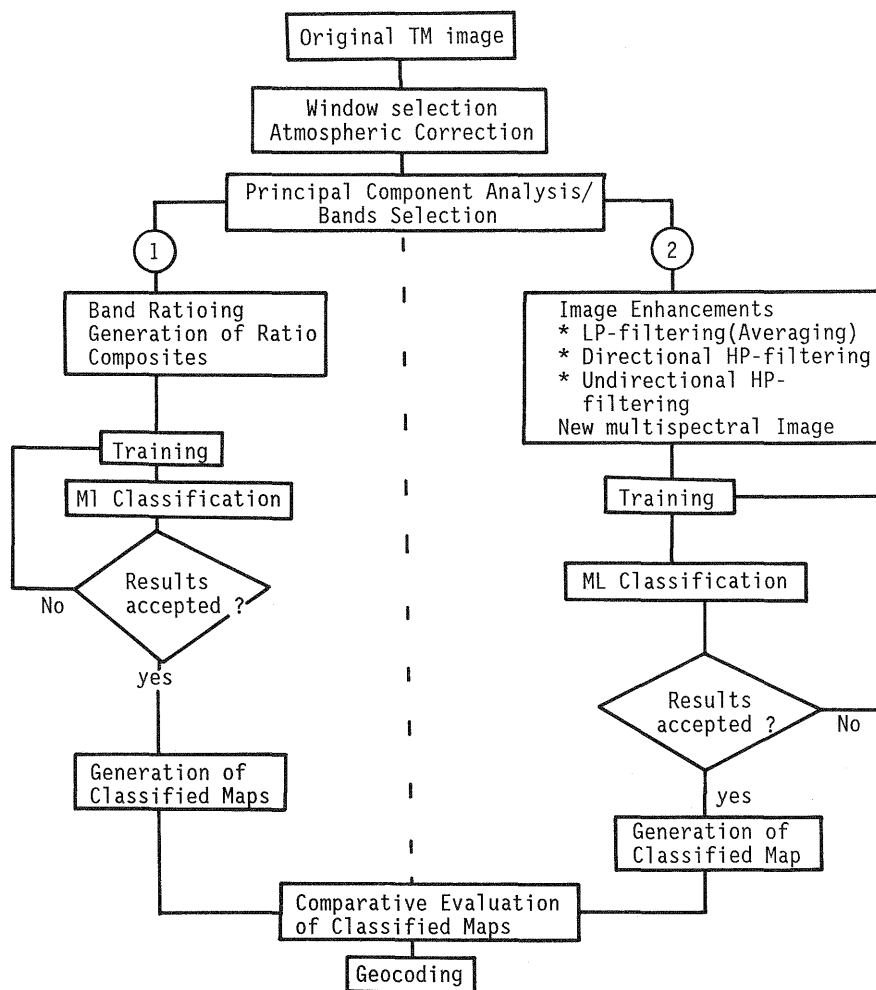


Fig.3 Flow chart of adopted Procedure

$$\text{Ratio composite 1 (TR1)} = \begin{pmatrix} \text{bd1} & \text{bd1} & \text{bd1} \\ \text{---} & \text{---} & \text{---} \\ \text{bd3} & \text{bd4} & \text{bd7} \end{pmatrix}$$

$$\text{Ratio composite 2 (TR2)} = \begin{pmatrix} \text{bd3} & \text{bd3} & \text{bd3} \\ \text{---} & \text{---} & \text{---} \\ \text{bd1} & \text{bd4} & \text{bd7} \end{pmatrix}$$

$$\text{Ratio composite 3 (TR3)} = \begin{pmatrix} \text{bd4} & \text{bd4} & \text{bd4} \\ \text{---} & \text{---} & \text{---} \\ \text{bd1} & \text{bd3} & \text{bd7} \end{pmatrix}$$

$$\text{Ratio composite 4 (TR4)} = \begin{pmatrix} \text{bd7} & \text{bd7} & \text{bd7} \\ \text{---} & \text{---} & \text{---} \\ \text{bd1} & \text{bd3} & \text{bd4} \end{pmatrix}$$

These 4 ratio combinations were selected after visual analysis of all the possible combinations generated from the chosen bands.

#### 4.4 Enhancement

Spatial filtering was used to generate another multispectral image, which was assigned the name TAH. For this purpose all the selected bands of the original image were passed through a combination of LP-filtering, directional HP-filtering of one-dimensional high energy areas and undirectional HP-filtering of other energy areas. These operations emphasised edges, lines and smoothed areas of homogeneity in the image. GOP 302 image processing program ENHANCE was used for this

purpose. This program uses three standard kernel sets. Each set consists of two complex-valued kernels. The real part of the first kernel performs low-pass filtering, while the imaginary part performs isotropic high-pass filtering. The second kernel performs two non-isotropic high-pass filtering in two different orientations, separated by 90 degrees (GOP 302 image processing manual).

#### 4.5 Training sites

Training sites were selected from all the images (both the ratio composites and the enhanced image). A total of 7 landcover classes were identified (table 1). All the training sites were extracted with the aid of interpreted aerial photographs of the area. Other ancillary information were also used. GOP 302 image processing program STAT was used to extract the statistics for each class from each of the images.

Table 1. Landcover classification hierarchy

S/No.	Landcover class
1.	Water
1.1	Clear water
1.2	Muddy water (with vegetation in some areas)
2.	Vegetation
2.1	Shrubland

- 2.2 Grass Savanna
- 3. Barrenland
- 3.1 Bare rocky surfaces
- 3.2 Sandy surfaces
- 3.3 Bare rainfed flood plains
- 3.4 Mixed barren areas

#### 4.6 Classification

A maximum likelihood classification was applied to each of the ratio composites and to the enhanced image, resulting in 5 classified landcover maps

#### 4.7 Classification assessment

To assess the classification accuracy of each image, a pixel by pixel comparison of each of the classification results and an assumed true map, based on confusion analysis was made. The true map was obtained also with the aid of the aerial photographs and contains selected test areas different from the training sites used in the classification. These test areas were assigned names corresponding to the classes, prior to classification. Statistics were extracted from them and then overlapped with each of the classification results. This gave a pixel by pixel comparison of the two maps. It showed the number of pixels of each class that were correctly classified. Errors of omission and commission were calculated for each class in each of the classified maps according to the methods illustrated by Jenson (1986). Prior to classification an overall accuracy of 90% was set as a threshold in assessing the performance of the images. Table 2, (a to e) show the error matrices for each of the classified images. A summary of the performance of each image is presented in table 3.

### 5. GEOCODING

A total of 55 control points were selected from the original image. These same points were identified on the topographic maps (1:50 000) and their UTM coordinates extracted. Both the image coordinates (row and column) and the map coordinates were the input data in computing the parameters of affine transformation, which was used to rectify the imagery to the UTM frame. The computation was based on the first order polynomial equations fit to the control point data using least-squares criteria (Konecny and Lehmann 1984, Jenson 1986, LaBash and Civco 1989 and Karl Kraus 1990). Usually first order polynomial is enough to model the translation and the scale changes in x and y axes, skew and rotation for a small area of TM scene (Jenson 1986). Moreover the area under investigation is relatively flat.

To determine how well the coefficients obtained from the least-squares regression accounted for the geometric distortion in the input image, a root mean square error (RMSE) was computed for each control point (Jenson 1986, LaBash and Civco 1989). Prior to this a maximum RMSE of 0.90 was set as a threshold. Control points were systematically reduced until a total of 30 points produced an acceptable result. These 30 points were used to compute the final transformation parameters used to

geocode each of the classified maps to the UTM grid. A nearest-neighbour interpolation was used to resample the pixel values of the input images.

### 6. DISCUSSION AND CONCLUSION

In terms of the overall accuracy, all the images performed well above the classification accuracy of 90% set as a threshold prior to classification. However the 4th ratio composite - TR4 provided the best overall accuracy of 93.3%. 2nd and 3rd composites provided the next best overall result - The overall accuracy was lowest in the enhanced image TAH. For the individual classes, the percentage agreement was highest in class barren1 (bare rocky surfaces). The ratio composites represented this class with 98.8% agreement, while the enhanced image represented it with 99.5%. This class was easily separable spectrally from other classes, which accounted for the high representation by all the images. The percentage agreement was lowest in the class barren3 (bare flood plains), with a representation of between 75.8% and 77% by the ratio composites and 79.5% by the enhanced image. The omission error from all the images was relatively high in this class. This was due to the difficulty in spectral separation of this class from other barrenland classes, particularly barren2 and barren4. Merging the barrenland classes into one class will certainly improve the situation. Clear water was also not very well represented by the ratio composites. They all had 85.9% agreement. The enhanced image TAH did relatively better with 96.9%. The class shrubland was highly represented by all the images with over 97% in the ratio composites and a little over 98% in the enhanced image TAH. Turbid water was also well represented with the agreement highest in TAH - 97.2%. Grass savanna was well represented by the ratios, but poorly represented by the enhanced image TAH with 85.0%.

In conclusion, the following deductions can be made.

- i) At the level of classification discussed above all the images provided acceptable results. However the ratio composite TR4 had the best overall result. The ratio composites also highlighted the vegetation very well.
- ii) The enhanced image TAH performed better than the ratio composites in 5 of the classes - water1, water2, shrubland, barren1 and barren3. It showed that if the sub-classes are merged together, this image will probably provide a better result than all the ratios.
- iii) All the images so formed can provide acceptable results if used in change detection. However enhanced image TAH, which represented much of the individual classes better might be more suitable for use in change detection studies in this region.

### 7. REFERENCES

1. Aronoff, S. 1982. Classification Accuracy: A user Approach. Photogrammetric Engineering and Remote Sensing, 48, pp 1299-1307.
2. Bernstein, R. 1983. Image Geometry and Rectification. Manual of Remote Sensing, ASPRS, Vol 1, pp 875-881.
3. Campbell, J. B. 1981. Spatial correlation effe-

Table 2. Error analysis of the classified maps with test data  
a/ TR1

Actual Land classes	Classified map								Total	Omi. error (%)	Com. error (%)	Accuracy (%)
	1	2	3	4	5	6	7	8				
1. Water1	55	4	0	0	0	5	0	0	64	14.1	17.2	85.9
2. Water2	6	135	0	0	0	0	0	1	142	4.9	2.8	95.1
3. Shrubland	1	0	434	0	0	0	0	12	447	2.9	0.0	97.1
4. Grass Savanna	0	0	0	356	7	3	1	5	372	4.3	5.6	95.7
5. Barren1	0	0	0	0	752	0	9	0	761	1.2	3.5	98.8
6. Barren2	0	0	0	10	5	263	3	12	293	10.2	20.5	89.8
7. Barren3	2	0	0	10	15	39	252	13	331	23.9	6.3	76.1
8. Barren4	2	0	0	1	0	13	8	209	233	10.3	18.5	89.7
Total	64	142	447	372	761	293	331	233	2643	Overall accuracy = 92.9%		

b/ TR2

Actual Land classes	Classified map								Total	Omi. error (%)	Com. error (%)	Accuracy (%)
	1	2	3	4	5	6	7	8				
1. Water1	55	4	0	0	0	5	0	0	64	14.1	15.6	85.9
2. Water2	5	136	0	0	0	0	0	1	142	4.2	2.8	95.8
3. Shrubland	1	0	434	0	0	0	0	12	447	2.9	0.0	97.1
4. Grass Savanna	0	0	0	358	6	3	1	4	372	3.8	5.6	96.2
5. Barren1	0	0	0	0	752	0	9	0	761	1.2	3.3	98.8
6. Barren2	0	0	0	10	5	260	3	15	293	11.3	19.5	88.7
7. Barren3	2	0	0	10	14	40	252	13	331	23.9	6.3	76.1
8. Barren4	2	0	0	1	0	9	8	213	233	8.6	19.3	91.4
Total	64	142	447	372	761	293	331	233	2643	Overall accuracy = 93.1%		

c/ TR3

Actual Land classes	Classified map								Total	Omi. error (%)	Com. error (%)	Accuracy (%)
	1	2	3	4	5	6	7	8				
1. Water1	55	4	0	0	0	5	0	0	64	14.1	12.5	85.9
2. Water2	3	138	0	0	0	0	0	1	142	2.8	2.8	97.2
3. Shrubland	1	0	437	0	0	0	0	9	447	2.2	0.0	97.8
4. Grass Savanna	0	0	0	356	7	2	2	5	372	4.3	5.9	95.7
5. Barren1	0	0	0	9	752	0	0	0	761	1.2	3.5	98.8
6. Barren2	0	0	0	11	5	258	3	16	293	11.9	18.8	88.1

7. Barren3	2	0	0	10	15	40	251	13	331	24.2	6.9	75.8
8. Barren4	2	0	0	1	0	8	9	213	233	8.6	18.9	91.4
Total	64	142	447	372	761	293	331	233	2643	Overall accuracy = 93.1%		

d/ TR4

Actual Land cover	Classified map								Total	Omi. error (%)	Com. error (%)	Accuracy (%)
	1	2	3	4	5	6	7	8				
1. Water1	55	4	0	0	0	5	0	0	64	14.1	15.6	85.9
2. Water2	5	136	0	0	0	0	0	1	142	4.2	2.8	95.8
3. Shrubland	1	0	434	0	0	0	0	12	447	2.9	0.0	97.1
4. Grass savanna	0	0	0	356	6	4	1	5	372	4.3	4.8	95.7
5. Barren1	0	0	0	0	752	0	9	0	761	1.2	3.4	98.8
6. Barren2	0	0	0	7	5	268	3	10	293	8.5	19.8	91.5
7. Barren3	3	0	0	10	15	35	255	13	331	23.0	6.3	77.0
8. Barren4	1	0	0	1	0	14	8	209	233	10.3	17.6	89.7
Total	64	142	447	372	761	293	331	233	2643	Overall accuracy = 93.3%		

e/ TAH

Actual Land classes	Classified map								Total	Omi. error (%)	Com. error (%)	Accuracy (%)
	1	2	3	4	5	6	7	8				
1. Water1	62	2	0	0	0	0	0	0	64	3.1	23.4	96.9
2. Water2	3	139	0	0	0	0	0	0	142	2.1	1.4	97.9
3. Shrubland	0	0	439	0	0	0	0	8	447	1.8	1.1	98.2
4. Grass savanna	0	0	1	316	0	7	15	33	372	15.1	6.7	84.9
5. Barren1	0	0	0	0	757	0	4	0	761	0.5	2.5	99.5
6. Barren2	0	0	0	12	0	259	8	14	293	11.6	11.3	88.4
7. Barren3	10	0	1	3	19	18	263	17	331	20.5	12.1	79.5
8. Barren4	2	0	3	10	0	8	13	197	233	15.5	30.9	84.5
Total	64	142	447	372	761	293	331	233	2643	Overall accuracy = 92.0%		

Table 3. Summary of accuracy

Images	TR1 (%)	TR2 (%)	TR3 (%)	TR4 (%)	TAH (%)
1. Water1	85.9	85.9	85.9	85.9	96.9
2. Water2	95.1	95.8	97.2	95.8	97.9

3. Shrubland	97.1	97.1	97.8	97.1	98.2
4. Grass savanna	95.7	96.2	95.7	95.7	85.0
5. Barren1	98.8	98.8	98.8	98.8	99.5
6. Barren2	89.8	88.7	88.1	91.5	88.4
7. Barren3	76.1	76.1	75.8	77.0	79.5
8. Barren4	89.7	91.4	91.4	89.7	84.5
Overall accuracy	92.9	93.1	93.1	93.3	92.0

- cts upon accuracy of supervised classification of land cover. Photogrammetric Engineering and Remote Sensing, 47, pp 355-357.
- Carr, J.R., C.E. Glass, and R.A. Schowengerdt. 1983. Signature Extension versus Retraining for multispectral classification of Surface mines in Arid Regions. Photogrammetric Engineering and Remote Sensing, 49, pp 1193-1199.
  - Chalmers, A.I. and R. Haris. 1981. Band ratios in multispectral analysis of Landsat digital data. Proceedings of 8th Annual Conference of the Remote Sensing Society, pp 139-146.
  - Congalton, R.G., Oderwald, R. and R. Mead. 1983. Landsat classification accuracy using multivariate statistical techniques. Photogrammetric Engineering and Remote Sensing, 49, pp 1671 - 1678.
  - Dech, W.S. 1987. Erfassung der Landnutzungsstrukturen nordwestlich Würzburg anhand digitaler, multispektraler Landsat 5 TM Daten. Technical Report, DFVLR-FB 87-37.
  - Dreiser, C. 1988. Anwendbarkeit von Landsat (TM und MSS) Daten für eine Weidelandinventur in semi-ariden und ariden Räumen am Beispiel Nord Kenya. Technical Report. DFVLR-FB 88-18.
  - Duda, R.D. and P.E. Hart. 1973. Pattern classification and scene analysis. John Wiley and Sons Inc, New York.
  - Estes, J.E., E.J. Hajic, and L.R. Tinney. 1983. Fundamentals of Image Analysis: Analysis of visible and Thermal infrared data. Manual of Remote Sensing, ASPRS, Vol 1, pp 1039-1040.
  - Fung, T., LeDrew, E. 1987. Application of principal component analysis to change detection. Photogrammetric Engineering and Remote Sensing. Vol. 53, 12, pp 1649-1658.
  - Gesellschaft für Angewandte Fernerkundung. 1990 Bericht zu den Projekten- Thematische Kartierungen Mayo - Kebbi und Ouaddai Biltine, Tchad. Munich, Germany. pp 35-46.
  - GOP 302 Image processing Manual. CONTEXTVISION AB, Linköping, Sweden.
  - Haralick, R.M., and K. Fu. 1983. Pattern Recognition and Classification. Manual of Remote Sensing, ASPRS, Vol 1, pp 793-805.
  - Hill, J., and J. Megier. 1986. Rural Landuse inventory and mapping in the Ardeche area using multitemporal TM data. International Geoscience and Remote Sensing symposium, 2, pp 1135-1141.
  - Ingebristen, S.E. and R.J.P. Lyon. 1985. Principal component analysis of multitemporal image pairs. International Journal of Remote Sensing, 6, pp 687-696.
  - Ioka, M., and M. Koda. 1986. Performance of Landsat 5 TM data in landcover classification. International Journal of Remote Sensing, 7, 12, pp 1715-1728.
  - Irons, J.R., B.L. Markham, R.F. Nelson, D. Toll, and D.L. Williams 1985. The effects of spatial resolution on the classification of TM data. 1985. International Journal of Remote Sensing, 6, pp 1385-1403.
  - Jenson, J.R. 1986. Introductory Digital Image processing. Prentice-Hill, Englewood Cliffs, New Jersey, pp 94-225.
  - Konecny, G. and G. Lehmann. 1984. Photogrammetrie. Walter de Gruyter, Berlin, pp 301 -323.
  - Kraus, K. 1990. Fernerkundung. Ferd. Dummlers Verlag. Bonn, Vol 2, pp 376-562.
  - LaBash, C.L. and D.L. Civco. 1989. The use of linearly transformed Landsat TM data in landuse and landcover classification. Technical Papers, 1989 ASPRS/ACSM Annual Convention. Baltimore.
  - Lo, T.H., F.L. Scarpace, and T. M. Lillesand. 1986. Use of multitemporal spectral profiles in agricultural landcover classification. Photogrammetric Engineering and Remote Sensing, 52, 4, pp 535-544.
  - Majumdar, T.J., B.B. Bhattacharya, S. Tanaka, and A. Rikimaru. 1991. Landuse classification for a part of Kamiichi Area, Japan, using Visible, IR and Thermal IR data. Geocarto International (2), pp 39-44.
  - Pinter, P.J., G. Zipoli, G. Maracchi, and R.J. Reginato. 1987. Influence of topography and sensor view angles on NIR/RED ratios and greenness vegetation indices of wheat. International Journal of Remote Sensing, 8, 6, pp 953-957.
  - Schumacher, H. 1991. Untersuchungen zur überwachten Klassifikation von Fernerkundungsaufnahmen. Technical Report 169, Fachrichtung Vermessungswesen der Universität Hannover.